Depletion of Alveolar Macrophages Does Not Prevent Hantavirus Disease Pathogenesis in Golden Syrian Hamsters

Christopher D. Hammerbeck[a], Rebecca L. Brocato[a], Todd M. Bell[b*Δ], Christopher W. Schellhase[bΔ], Steven R. Mraz[c†], Laurie A. Queen[a‡], Jay W. Hooper[a]

[a]Virology Division, United States Army Medical Research Institute of Infectious Diseases (USAMRIID), Ft. Detrick, Maryland, United States of America

[b]Pathology Division, United States Army Medical Research Institute of Infectious Diseases (USAMRIID), Ft. Detrick, Maryland, United States of America

[c]Veterinary Medicine Division, United States Army Medical Research Institute of Infectious Diseases (USAMRIID), Ft. Detrick, Maryland, United States of America

Running Head: Depletion of AMθ in ANDV-infected hamsters

#Address correspondence to Jay W. Hooper, jay.w.hooper.civ@mail.mil

*Present address: Todd M. Bell, National Center for Biodefense and Infectious Diseases, George Mason University, Fairfax, Virginia

† Present address: Steven R. Mraz, Military Personnel Division, Wiesbaden, Germany

‡ Present address: Laurie A. Queen, Southern Research Institute, Frederick, Maryland

Δ Both authors contributed equally to this work.

Word count abstract: 199 (Abstract); 150 (Importance); 6,358 (Text)

ABSTRACT

Andes virus (ANDV) is associated with a lethal vascular leak syndrome in humans termed hantavirus pulmonary syndrome (HPS). The mechanism for the massive vascular leakage associated with HPS is poorly understood, however dysregulation of components of the immune response is often suggested as a possible cause. Alveolar macrophages are found in the alveoli of the lung and represent the first line of defense to many airborne pathogens. To determine whether alveolar macrophages play a role in HPS pathogenesis, alveolar macrophages were depleted in an adult rodent model of HPS that closely resembles human HPS. Syrian hamsters were treated, intratracheally, with clodronate-encapsulated liposomes or control liposomes and were then challenged with ANDV. Treatment with clodronate-encapsulated liposomes resulted in significant reduction in alveolar macrophages but depletion did not prevent pathogenesis or prolong disease. Depletion also did not significantly reduce the amount of virus in the lung of ANDV-infected hamsters but altered neutrophil recruitment, MIP-1α and MIP-2 chemokine expression and VEGF levels in hamster BAL early after intranasal challenge. These data demonstrate that alveolar macrophages may play a limited protective role early after exposure to aerosolized ANDV, but do not directly contribute to hantavirus disease pathogenesis in the hamster model of HPS.

IMPORTANCE

Hantaviruses continue to cause disease worldwide for which there are no FDA licensed vaccines, effective post-exposure prophylactics or therapeutics. Much of this can be attributed to a poor understanding of the mechanism of hantavirus disease pathogenesis. Hantavirus

disease has long been considered an immune-mediated disease; however, by directly manipulating the Syrian hamster model, we continue to eliminate individual immune cell types. As the most numerous immune cell present in the respiratory tract, alveolar macrophages are poised to defend against hantavirus infection; but, those antiviral responses may also contribute to hantavirus disease. Here, we demonstrate that, like our prior T and B cell studies, alveolar macrophages neither prevent hantavirus infection nor cause hantavirus disease. While these studies reflect pathogenesis in the hamster model, they should help us rule-out specific cell types and prompt us to consider other potential mechanisms of disease in an effort to improve the outcome of human HPS.

INTRODUCTION

Hantaviruses are enveloped members of the family *Bunyaviridae* that contain a tri-segmented, negative-sense, single-strand RNA genome. The three gene segments, L, S, and M encode the RNA polymerase, nucleoprotein, and envelope glycoproteins (G1 and G2), respectively. While these pathogens are carried chronically and asymptomatically in rodent hosts, in humans, hantaviruses cause two unique vascular-leak syndromes that cover a spectrum of severity ranging from proteinuria to pulmonary edema and frank hemorrhage(1-4). Old-World hantaviruses, including Puumala virus (PUUV), Dobrava virus (DOBV), Seoul virus (SEOV), and Hantaan virus (HTNV), have been associated with a mild-to-severe disease, hemorrhagic fever with renal syndrome (HFRS). HFRS has a case-fatality rate between <0.1% to 15% and is characterized by fever, vascular leakage resulting in hemorrhagic manifestations and

renal failure. New-World hantaviruses have been associated with a highly lethal disease, hantavirus pulmonary syndrome (HPS). HPS caused by the most prevalent North American and South American hantaviruses, Sin Nombre virus (SNV) and Andes virus (ANDV), respectively, has a case-fatality rate or 30-50% and is characterized by fever and vascular leakage resulting in non-cardiogenic pulmonary edema followed by shock. Hantaviruses alter the barrier properties of the microvascular endothelial cells that they infect, causing vascular leakage in the kidneys or lungs (5). The specific mechanism underlying this endothelium dysfunction remains unknown, but hantavirus infection of endothelial cells is nonlytic, suggesting that other, possibly host derived factors, renders the endothelium unable to regulate barrier integrity, leading to pulmonary edema (6).

While hantaviruses are known to cause disease by multiple routes of infection(5), the predominant route of human exposure is thought to be inhalation of excreta from infected rodent hosts (reviewed in references (6) and (7)) suggesting that cells in the alveoli may play an important role in clearing, or alternatively, contributing to disease caused by aerosolized hantaviruses. Alveolar macrophages (AMθ) are found in the alveoli and alveolar ducts of the lung and represent the first line of defense to many airborne pathogens(8). Not only are they crucial regulators of immune system activity through their secretion of either pro- or anti-inflammatory cytokines, but they are vitally important in the maintenance and remodeling of lung tissue via the production of growth factors, cytokines and proteinases. Activated AMθ are known to provide a critical element of protection against pathogens(9, 10) by releasing chemokines that recruit other innate immune cell types to areas of infection and secreting antiviral cytokines. However, activation of AMθ, can also contribute to pathology by releasing

the same cytokines that are important in providing protection from pathogens(11-14). Alveolar macrophages secrete multiple cytokines when activated including IL-1, IL-6, IL-8, TGF-β, inducible nitric oxide synthase (iNOS), and TNFα. Notably, the production of TNFα further upregulates the release of other proinflammatory cytokines such as IL-1β, IL-6, and IL-8 which contribute to the initiation of adaptive immune responses(15). While these cytokines and chemokines act locally to choreograph immune responses that are important for protection against pulmonary pathogens, a number of these cytokines have been shown to promote vascular permeability and pulmonary edema that are the hallmarks of pathogenic hantavirus infection (16-20). Correspondingly, studies of humans infected with hantavirus have detected high titers of proinflammatory and vasoactive cytokines in lung tissue of hantavirus pulmonary syndrome (HPS) patients and high numbers of cytokine producing cells correlated with the severity of HPS pathology (21). Moreover, systemic levels of inflammatory cytokines have also been reported in plasma of patients with hemorrhagic fever with renal symptoms (HFRS) (22) suggesting a role for these cytokines in disease pathogenesis.

Alveolar macrophages are known to be permissive to hantavirus infection(23, 24) but do not appear to be primary targets of infection as hantavirus replication in alveolar macrophages is less efficient than in endothelial cells. Furthermore, AMθ have been found to be associated with hantavirus antigen in cases of human HPS(25) caused by SNV or in cases of "European HPS" following PUUV infection(26) but it isn't clear if that is a result of direct infection of alveolar macrophages or as a result of phagocytosis. Despite these associations, hantavirus infection of human AMθ induced only modest antiviral responses and cell culture supernatants from SNV infected AMθ failed to cause increased permeability of endothelial cell

monolayers(24) suggesting that soluble mediators secreted by infected AMθ do not contribute to hantavirus disease.

ANDV causes a lethal disease in adult Syrian hamsters (27) that resembles HPS in humans including the clinical signs including severe dyspnea, rapid progression from first signs to death, fluid in the pleural cavity; the histopathology in the lungs and spleen; and the viral incubation period(28). To determine if AMθ contribute to hantavirus disease in hamsters, we depleted AMθ using clodronate-encapsulated liposomes, delivered prior to ANDV challenge. Clodronate treatment significantly reduced the percent and number of AMθ in hamster bronchial alveolar lavage (BAL) during intramuscular and intranasal ANDV challenge but had little effect on disease pathogenesis. Depletion did result in a slightly more rapid and uniform disease course during intranasal infection suggesting that AMθ may provide some protection against exposure to airborne ANDV but overall, these data suggest that AMθ do not directly contribute to hantavirus disease pathogenesis in the Syrian hamster model of human hantavirus pulmonary syndrome.

MATERIALS AND METHODS

Virus, cells, and medium. ANDV strain Chile-9717869 (27) was propagated in Vero E6 cells (Vero C1008, ATCC CRL 1586). Preparation of twice-plaque-purified ANDV stock has been described previously(27). Cells were maintained in Eagle's minimum essential medium with Earle's salts containing 10% fetal bovine serum, 10 mM HEPES, pH 7.4, penicillin-streptomycin (Invitrogen) at 1×, and gentamicin sulfate (50 μg/ml) at 37°C in a 5% CO_2 incubator.

Challenge with hantavirus. Female Syrian hamsters 6 to 8 weeks of age (Harlan, Indianapolis, IN) were anesthetized by inhalation of vaporized isoflurane using an IMPAC 6 veterinary anesthesia machine. For intramuscular (i.m.) challenges, anesthetized hamsters were injected with 80 PFU (10 LD_{50}) of virus diluted in PBS (0.2 ml, caudal thigh) delivered with a 1-ml syringe with a 25-gauge, five-eighths-inch needle. For intranasal (i.n.) challenges, anesthetized hamsters were administered 50 µl delivered as 25 µl per nare with a plastic pipette tip (4,000 PFU ANDV total, 42 LD_{50}). Groups of 8 hamsters were typically used for experimental treatments, unless otherwise stated. All work involving hamsters was performed in an animal biosafety level 4 (ABSL-4) laboratory. Hamsters were observed two to three times daily.

Macrophage depletion. Clodronate-encapsulated liposomes (Clodrosome – 5mg/ml clodronate) and control PBS-encapsulated liposomes (Encapsome) were purchased from Encapsula Nano Sciences. Hamsters were anesthetized using 0.2 ml / 100g rat KAX (ketamine-acepromazin-xylazine) administered by i.m. injection. Each animal was then placed in a dorsal recumbent position and an otoscope (Welch Allyn) was used visualize the vocal folds. The vocal folds were numbed by topically administering a 2% Lidocaine HCl jelly (Akorn) and then a 16G x 1¼" Surflo catheter (Terumo) was passed between the vocal folds. Hamsters were then treated with either 0.2 ml Clodrosome or 0.2 ml Encapsome by attaching a loaded syringe to the catheter and aspirating the contents into the lung.

Flow cytometry analysis. Hamsters were deeply anesthetized (0.4 ml Rat KAX / 100g) and then extensively perfused with sterile saline (Baxter) before being euthanized. To isolate alveolar macrophages, animals were placed in a dorsal recumbent position, then a midline neck incision

was made and dissected down carefully so that the trachea was exposed. A second incision was made near the xyphoid process then scissors were used to carefully remove the rib cage exposing the lungs ensuring not to damage the lungs in the process. A 16g x 1 ¼" catheter was inserted into the trachea and the lungs were lavaged 3 times using 1 ml of a 0.02% EDTA solution. BAL samples were then centrifuged at 514 x g for 5 minutes. Cells were then collected and washed twice in PBS containing 2% FBS. In some experiments, cells were incubated at 4° C for 15 min in a blocking buffer consisting of PBS containing 2% FBS and 2% normal rat serum (Sigma–Aldrich) prior to staining with antibody. Approximately 10^6 cells were stained with mouse-anti-hamster MARCO(29) (clone PAL-1; 10μg/100μl; AbD Serotec) followed by anti-mouse IgM (clone RMM-1; 0.4μg/ml; BioLegend) for 15-20 min at 4° C. Stained cells were then were fixed in Cytofix buffer (BD Biosciences) for 15 min at 4°C before being analyzed on a FACSCalibur™ flow cytometer (BD Biosciences) using CellQuest software (BD Biosciences) or FACSCanto™ II flow cytometer (BD Biosciences) using FACsDiva software (BD Biosciences). AM and neutrophil cell numbers in BAL preparations were mathematically determined by comparing cell numbers to numbers of PKH26 reference microbeads (Sigma) using the formula: # cells/ml = (# cell events x dilution factor/# bead events x dilution factor) x # beads/ml. Data were analyzed using FlowJo software (Treestar).

Plaque assay. Hantavirus plaque assays were performed as previously described(30).

Isolation of RNA and real-time PCR. Approximately 250 mg of lung tissue was homogenized in 1.0 ml TRIzol reagent using gentleMACS M tubes and a gentleMACS dissociator on the RNA

setting. RNA was extracted from TRIzol samples as recommended by the manufacturer. The concentration of the extracted RNA was determined using a NanoDrop 8000 instrument and raised to a final concentration of 10 ng/µl. Real-time PCR was conducted on a Bio-Rad CFX thermal cycler using an Invitrogen Power SYBR green RNA-to-C_T one-step kit according to the manufacturer's protocols. Primer sequences are as follows (26): ANDV S 41F, 5' - GAA TGA GCA CCC TCC AAG AAT TG - 3'; ANDV S 107R, 5' - CGA GCA GTC ACG AGC TGT TG - 3'. Cycling conditions were 30 min at 48°C, 10 min at 95°C, and 40 cycles of 15 s at 95°C and 1 min at 60°C. Data acquisition occurred following the annealing step.

Hamster cytokine ELISAs.

Anti-hamster MIP-1α (MBS033532), MIP-2 (MBS006761), TNFα (MBS046042) and VEGF-A (MBS024541) ELISA ELISA kits were purchased from MyBioSource and were used according to the manufacturer's recommendations.

Preparation of tissues for histology. Tissues were fixed in 10% neutral buffered formalin, trimmed, processed, embedded in paraffin, cut at 5 to 6 µm, and stained with hematoxylin and eosin (H&E) for histopathology analysis. To determine the presence of ANDV antigens in association with alveolar macrophages or colocalized with endothelial cells, serial sections were then stained as follows. For ANDV immunohistochemistry, a monoclonal antibody (USAMRIID#1244) against ANDES virus was used on all tissue slides. Normal mouse IgG was used as the negative serum control for the control slides. Briefly, the unstained sections were deparaffinized, rehydrated, and pretreated with Tris/EDTA buffer for 30 minutes at 95-100°C. Slides were rinsed and a serum free protein block with 5% horse serum was applied for 30

minutes. The monoclonal antibody was then applied to the tissue at a dilution of 1:1200 and incubated for 1 hour at room temperature. The slides were then treated with alkaline phosphatase labeled secondary mouse IgG antibody (Vector Labs, Burlingame, CA. cat# MP-5402) for 30 minutes at room temperature. All slides were exposed to ImmPACT Vector® Red (Vector Labs, Burlingame, CA. cat# SK-5105) substrate-chromagen for 30 minutes, rinsed, counterstained with hematoxylin, dehydrated and cover-slipped with Permount®(Fisher,cat# SP15-500). For CD31 immunohistochemistry, an immunoperoxidase assay was performed using a rabbit anti-CD31 polyclonal antibody (Abcam; cat# ab28364). A normal rabbit IgG was used as the negative serum control for the control slides. Briefly, the unstained sections were deparaffinized, rehydrated, subjected to a methanol hydrogen peroxide block, rinsed and pretreated with Tris/EDTA buffer for 30 minutes at 95-100°C. Slides were rinsed and a serum free protein block with 5% goat serum was applied for 30 minutes. The polyclonal antibody was then applied to the tissue at a dilution of 1:75 and incubated overnight at room temperature. The slides were then treated with the EnVision horseradish peroxidase labeled secondary antibody (Dako, Carpinteria, CA, cat# K4007) for 30 minutes at room temperature. All sections were exposed to a DAB (3,3-diaminobenzidine) substrate-chromagen for 5 minutes, rinsed, counterstained with hematoxylin, dehydrated and cover-slipped with Permount.

Statistical analysis. Survival curves were compared with Kaplan-Meier survival analysis with log-rank comparisons and Dunnett's correction. Comparisons of viral genome, infectious virus, alveolar macrophage and neutrophil percent and number, and ELISA cytokine titers were done using a one-way analysis of variance (ANOVA) with Tukey's multiple-comparison test. P values

of less than 0.05 were considered significant. Analyses were conducted using GraphPad Prism (version 5).

Ethics statement. Research at U.S. Army Medical Research Institute of Infectious Diseases (USAMRIID) was conducted under an Institutional Animal Care and Use Committee (IACUC) approved protocol in compliance with the Animal Welfare Act, PHS Policy, and other federal statutes and regulations relating to animals and experiments involving animals. The facility where this research was conducted is accredited by the Association for Assessment and Accreditation of Laboratory Animal Care, International and adheres to principles stated in the Guide for the Care and Use of Laboratory Animals, National Research Council, 2011.

RESULTS

Depletion of AMθ does not prevent disease following intramuscular ANDV challenge.

Clodronate has been used extensively to deplete AMθ in many animal models including the Syrian hamster (31). In the Syrian hamster, AMθ were identified as $FSC^{hi}SSC^{hi}$, MARCO expressing cells in hamster BAL fluid (Fig. **1A)** and intratracheal administration of clodronate encapsulated liposomes was found to effecively reduce the number of AMθ in hamsters during ANDV infection as determined by a reduction in either $MARCO^{+}$ cells (**Fig. 1B and 1D**) or $FSC^{hi}SSC^{hi}$ cells (**Fig. 1C and 1D**) and histolopathologic analysis of hamster lung tissue (**Fig. 1E**) during ANDV infection of hamsters. To begin to understand the role that AMθ play during ANDV disease pathogenesis, hamsters were treated intratracheally with clodronate

encapsulated liposomes (Clodrosome) or control PBS encapsulated liposomes (Encapsomes) on days -3 and -1. One group of hamsters was left untreated. Hamsters were then challenged with 80 pfu (10 LD_{50}) ANDV i.m. 10 days later, the number and percent of AMθ in hamster BAL were determined. Encapsome treatment did induce an increase in the number of alveolar macrophages (**Fig. 2A**) but by comparison, Clodrosome treatment resulted in a significant reduction in the total number of alveolar macrophages (**Fig. 2A**). Macrophage depletion did not prevent disease in hamsters (**Fig. 2B**) or significantly alter the mean time to death (Clodrosome = 12.88 days, Encapsome = 13.13 days, untreated = 11.38 days) The mean time to death following Encapsome treatment was significantly longer compared to untreated animals (13.13 days vs. 11.38 days; p=0.05) but not when compared to Clodrosome treated animals. Depletion of AMθ also did not result in increased ANDV titers in the lung as measured by PCR (**Fig. 2C**). These data suggest that despite becoming activated, AMθ are not important for protection against an intramuscular ANDV challenge nor do they contribute to disease pathogenesis following intramuscular challenge.

Serial sections of lung tissue from these groups further revealed the presence of ANDV antigen co-localized to CD31 positive endothelial cells in both capillaries and larger vessels (**Fig. 3A-3D**). Regardless of treatment, no differences were observed in the pathogenesis of HPS-like disease in ANDV-infected hamsters. Hamsters in all groups exhibited signs of mild to moderate inflammation, interstitial pneumonia, alveolar fibrin deposition and edema characteristic of ANDV infection.

Also noticed were multifocal foci of neutrophilic inflammation, along with mesothelial hypertrophy and atelectasis. The presence of necrotic/apoptotic debris was rare. Consistent

with the detection of viral genome by PCR, immunohistochemistry analysis revealed little to no difference in overall viral load within endothelial cells following clodrosome treatment. Interestingly, all identifiable alveolar macrophages found in ANDV infected hamsters were negative for Andes virus although positive cytoplasmic CD31 staining (**Fig. 3E**).

Depletion of AMθ **does not prevent disease following intranasal ANDV challenge**

Alveolar macrophages are more likely to be involved in the defense against airborne pathogens. To understand the protective or pathogenic responses that AMθ elicit to inhaled hantaviruses, AMθ were depleted prior to intranasal ANDV challenge. Groups of hamsters were treated intratracheally with Clodrosomes or control Encapsomes on days -3 and -1. One group of hamsters was left untreated. Hamsters were then challenged with 4000 pfu (42 LD_{50}) ANDV i.n. 10 and 17 days later, the number and percent of AMθ in hamster BAL were determined. Similar to what was seen after intramuscular challenge, 10 days after intranasal challenge the percentage and total number of AMθ in untreated or Encapsome treated animals were comparable (**Fig. 4A**). Encapsome treatment resulted in a trend towards increased numbers of AMθ compared to untreated animals but this difference was not significant. By comparison, Clodrosome treatment resulted in a significant reduction in both the percent and total number of AMθ. The percent of AMθ remained significantly reduced following clodrosome treatment 17 days after intranasal challenge (**Fig. 4B).** Surprisingly, though, was the observation that the number of AMθ at day 17 in the untreated group was significantly lower than the number of AMθ in the untreated group at day 10 (**Fig. 4C**). This phenomenon was only seen in the untreated groups as the number of AMθ in the Encapsome treated animals remained similar

between days 10 and 17. Although the total number of AMθ in the Clodrosome treated animals was lower on day 17 than on day 10, the difference between number of AMθ in the Clodrosome treated animals and untreated animals on day 17 was not significant. However, the difference in the number of AMθ in the Encapsome treated animals and untreated animals on day 17 was significant. The reduction in AMθ did not prevent disease in hamsters (**Fig. 4D**) but depletion did result in a more uniform and slightly more rapid disease course (mean time to death: Clodrosome = 14.75 days, Encapsome = 21.43 days, untreated = 19.13 days). ANDV titers in the lung were not significantly different in Clodrosome-treated hamster either day 10 or day 17 as determined by the presence of viral genome measured by PCR (**Fig. 4E**). However, there was a trend towards increased ANDV M copy number in the lungs of Clodrosome-treated animals 10 days post challenge.

TNFα levels in hamster BAL samples were significantly higher at the peak of disease compared to earlier time points (**Fig. 5A;** day 17 versus day 10) but AMθ depletion only affected TNFα expression early after infection. Interestingly, treatment with either Clodrosomes or control Encapsomes resulted in an increase in TNFα detected compared to untreated hamsters which could reflect the higher numbers of neutrophils and AMθ present in the BAL samples from these groups, respectively (**Fig. 4B and 6D**). The reduction in AMθ did not reduce the amount of TNFα detected in BAL samples 10 days after intramuscular challenge (**Fig. 5B**) which was similar to the amount of TNFα detected in BAL samples 10 day after intranasal challenge. Remarkably, TNFα levels at the peak of disease following intranasal challenge (day 17) were nearly twice that detected at the peak of disease following intramuscular challenge possibly reflecting the differences in AMθ activation when virus is administered directly to the lung.

These data suggest that AMθ do not contribute to disease pathogenesis but may contribute some degree of protection against following intranasal ANDV challenge.

Depletion of AMθ **alters neutrophil recruitment early, but not late, after intranasal ANDV challenge**

Alveolar macrophages coordinate many aspects of immune responses to airborne pathogens, including the recruitment of other immune cell types such as neutrophils. At the peak of hantavirus disease following intramuscular infection with ANDV (day 10), we observed a decrease in the neutrophil chemoattractant MIP-1α in BAL samples from AMθ depleted hamsters compared to untreated ANDV infected hamsters suggesting AMθ may be an important source of MIP-1α during hantavirus infection in the lung(**Fig. 6A**). However, the expression of the neutrophil chemoattractant MIP-2 in BAL samples from all hamsters remained unchanged(**Fig. 6B**), and, correspondingly, there was also little significant change in the number of neutrophils found in hamster BAL samples 10 days after intramuscular challenge (**Fig. 6C**). By comparison, when we investigated the role of AMθ in recruitment of neutrophils following intranasal challenge, we found that early in disease pathogenesis (day 10), MIP-1α and MIP-2 expression were reduced in both Clrodrosome and control Encapsome treated hamsters compared to untreated ANDV infected hamsters (**Fig. 6D and 6E**). We also found that Encapsome treatment resulted in increased numbers of recruited AMθ (**Fig. 4B**) while Clodrosome treatment resulted in an increased number of neutrophils (**Fig. 6F**). At the peak of disease following intranasal ANDV challenge (day 17), the expression of MIP-1α and MIP-2 was reduced approximately 50% compared to the expression seen on day 10. Moreover, the

expression of MIP-1α and MIP-2 was not dependent on treatment as equivalent amount of MIP-1α and MIP-2 were detected in BAL samples from all hamster (**Fig. 6D and 6E**). Neutrophil numbers were reduced in clodronate-treated animals by day 17 compared to numbers observed on day 10 but neutrophil numbers in the control Encapsome-treated and untreated hamsters remained virtually unchanged between days 10 and 17(**Fig. 6G**). In contrast, AMθ numbers in Encapsome-treated hamsters remained elevated on days 10 and 17 despite an overall drop in AMθ numbers in untreated hamsters (**Fig.4a and 4B**). These data suggest that AMθ may regulate neutrophil recruitment to the lung early after hantavirus infection but do not contribute significantly to neutrophil recruitment towards the peak of disease pathogenesis.

Depletion of AMθ **alters VEGF-A expression early after intranasal ANDV challenge**

Recently, vascular endothelial growth factor (VEGF) has been hypothesized to play a role in hantavirus disease pathogenesis. Moreover, AMθ are known sources of VEGF. We therefore asked whether VEGF expression in the lungs of hamsters infected with ANDV was dependent on the presence of AMθ. Compared to normal uninfected hamsters, VEGF-A expression in the BAL of hamsters 10 days after intranasal ANDV challenge was only slightly, but not significantly elevated (**Fig. 7**). Interestingly, at the time of peak disease on day 17, there was almost a two-fold increase in VEGF-A protein. Macrophage depletion did not further enhance VEGF-A in BAL samples late into infection (day17) as we observed no difference in VEGF titers in ANDV infected hamster BAL samples in the presence or absence of AMθ. However, when AMθ were depleted, VEGF-A expression in the BAL on day 10 was equivalent to the amount of VEGF-A detected in all hamster BAL samples on day 17. A similar increase in VEGF was observed in

Encapasome-treated hamsters. These data demonstrate that VEGF expression is enhanced in hamsters infected with ANDV but suggest that while AMθ may regulate the expression of VEGF by other cell types in the lung, they are not a major source of VEGF during hantavirus disease pathogenesis.

DISCUSSION

The human lung has a surface area of approximately 70m^2, and contains, on average, 480 million alveoli (32) which are in constant contact with the outside world. In this environment, homeostasis along the endothelial/epithelial boarder must be maintained to allow oxygen and carbon dioxide to freely exchange; however, these homeostatic mechanisms must remain pliable enough to allow immune responses to clear invading pathogens. Often considered the first line of defense against respiratory pathogens, the estimated 2 billion AMθ residing in the alveoli of the human lung(33) are uniquely juxtaposed to maintain lung homeostasis as well as orchestrate protection against airborne viruses and bacteria(34). In the case of hantaviruses, the predominant route of human exposure is thought to be inhalation of excreta from infected rodent hosts (reviewed in references (6) and (7)) suggesting that alveolar macrophages may play an important role in clearing, or alternatively, contributing to disease caused by aerosolized hantaviruses. Here, we demonstrate that alveolar macrophages play only a marginal role in protecting hamsters from lethal hantavirus infection but do not contribute to the disease caused by hantaviruses.

Alveolar macrophages contribute to the defense against many aerosolized pathogens, and in many cases, these responses are critical for host protection. In models of vaccinia virus, RSV and influenza virus infection, the depletion of alveolar macrophages results in greater viral replication and dissemination and an overall increase in the severity of infection (35-38). In some cases, the reduced levels of protection in the absence of alveolar macrophages is likely due to the impaired initiation of antiviral responses that result in abolished early cytokine and chemokine release and inhibited immune cell activation and recruitment (38, 39). In addition, Schneider et al (40) demonstrated that when alveolar macrophages were depleted in mice prior to infection with influenza virus, mice exhibited lower percent sO_2 and pO_2 pressure arguing that AMθ are important for maintaining lung function during infection. However, the same mechanisms that alveolar macrophages use to protect against pathogens have also been implicated in causing disease and increased vascular permeability in models of acute lung injury caused by infectious disease agents, such as human metapneumovirus (hMPV) (41) and Pseudomonas aeruginosa (42) as well as chronic obstructive pulmonary disease (COPD)(43) and nonischemic inflammatory lung injury (44). Alveolar macrophages may also serve as a reservoir for pathogens such as human metapneumovirus (hMPV) (41), measles virus(45) and *Legionella pneumophila*(46) and may indirectly contribute to the pathogenesis diseases caused by these pathogens by allowing for their replication and dissemination. Still, the enhancement of disease in the presence of alveolar macrophages may not always reflect a direct contribution by AMθ by way of proinflammatory cytokines or angiogenic factors but may indirectly be the result of increased immune cell recruitment by AMθ as seen in mouse models of mouse hepatitis virus type 1 (MHV-1) infection (47).

The role that AMθ play in disease caused by classical hemorrhagic fever viruses is less well understood. Alveolar macrophages express the primary and secondary receptors(48) for both hantaviruses (αvβ3 integrin(49) and complement receptor 3 and 4 (CR3 / CR4) (50)) and Ebola virus (DC-SIGN and DC-SIGNR(51)) and, corresponding, are known to be permissive to hantavirus (23, 24) and Ebola virus infection(52). However, in these cases, infection is less efficient or fails to induce a sustained inflammatory response compared to the primary targets of infection for these viruses and there is no evidence that hantavirus infection of AMθ induces apoptosis. Antigens of Yellow Fever virus, which is transmitted by the bite of the *Aedes aegypti mosquito,* can be found inside the rough endoplasmic reticulum and Golgi complex of AMθ, suggesting that viral replication can occur in these cells(53, 54) but it is unknown whether AMθ play any role in disease pathogenesis other than acting as a virus reservoir. Still, it is unknown whether other hemorrhagic fever viruses that commonly target monocyte lineage cells such as Dengue virus and Crimean Congo hemorrhagic fever virus target AMθ in a way that contributes to human disease. We failed to detect the presence of ANDV NP associated with hamster AMθ (Fig. 3E) suggesting that AMθ may only constitute a relatively minor target for hantaviruses and AMθ dysfuntion due to direct hantavirus infection is unlikely. Our analysis of ANDV NP associated with AMθ was limited to intramuscular challenge so it is possible that a greater associated may be seen following intranasal challenge. However, we see no difference in HPS pathology in hamsters following either i.n. or i.m. challenge. Moreover, our analysis was done at the peak of disease pathogenesis following i.m. challenge (Day 10) when ANDV NP staining of the lung endothelium was nearly continuous suggesting that the likelihood of ANDV / AMθ interactions would be as high as that following intranasal challenge.

How hamster AMθ respond to ANDV infection isn't entirely clear. Alveolar macrophages, in general, need to walk a fine line between homeostasis and host defense to protect the host while preventing catastrophic inflammation. One way AMθ contribute to lung protection is by phagocytizing most of the particulate matter that enters the lungs. This suggested that they may also contribute to the clearance of ANDV from the lungs of hamsters. Early after intranasal ANDV challenge we did see a trend toward increased detection of viral genome in hamsters that were depleted of AMθ although depletion of AMθ does not significantly alter the amount of live virus or viral genome detected in lung tissue late after infection (**Fig. 3E and 3F**). Hamsters devoid of AMθ also developed disease faster than untreated or control treated ANDV-infected hamsters. Interestingly, the highest number of surviving animals was found in encapsome-treated animals (**Fig. 3D**). Correspondingly, this group also had greater numbers of AMθ than clodronate-treated or untreated animals(**Fig. 3A-C**). Like other models, this could suggest that early after infection, AMθ help prevent the spread of infection by reducing infectious virus in the lung and by doing so may help control the rate at which disease pathogenesis progresses. At later times after infection, similar levels of viral genome and/or infectious virus was found in the lung of all hamsters arguing that AMθ contribute more substantially to the immune response against ANDV early after infection but less so at later times once ANDV is primarily replicating in endothelial cells. This is also consistent with the reduced numbers of AMθ detected on day 17 compared to day 10.

A second way AMθ contribute to lung protect is my modulating immune responses in the lung(34, 55). In the presence of harmless particulates such as dust, they may go as far as suppressing antigen-specific adaptive immune responses by either directly suppressing tissue-

resident T cells(56, 57) or by suppressing lung-resident dendritic cells(58), thus preventing them from migrating to draining lymph nodes and initiating immune responses. However, in the case of aerosolized pathogens, activation of AMθ results in a change in phenotype from a regulator of lung homeostasis to that of a cell capable of coordinating and participating in inflammatory immune responses (59, 60). Human AMθ make little TNFα when exposed to SNV compared to LPS (24) suggesting that hantavirus may be ineffective at activating AMθ. Correspondingly, we noticed little difference in the amount of TNFα in the BAL of hamsters in the presence or absence of AMθ following infection with ANDV intramuscularly (**Fig. 4A**) or at late times after intranasal infection (**Fig. 4B**). In the case of intramuscular infection, it's not clear whether AMθ would be effectively stimulated since it is assumed that infection of the endothelium would occur directly via the blood and not by inhalation. We did observe an increase in the amount of TNFα in BAL samples between day 10 and day 17 post-intranasal challenge indicating that an inflammatory response was occurring. However, at late times, depletion of macrophages did not reduce the amount of TNFα detected suggesting that AMθ are not a major source of TNFα that late in infection. Somewhat surprisingly, at early times (day 10) after intranasal challenge, the depletion of AMθ resulted in an increase in TNFα in BAL samples. One explanation is that in hamsters, AMθ are more prone to an immunosuppressive phenotype and by depleting them, other cell types including neutrophils, endothelial cells, T cells and epithelial cells are no longer prevented from producing TNFα. The fact that control Encapsome treated animals also had increased levels of TNFα may be reflected in the increased numbers of AMθ induced by Encapsome treatment. Resident AMθ at the time of Encapsome may retain their

immunosuppressive phenotype but any newly recruited AMθ could be expected to have a markedly different phenotype prior to adopting suppressive functions (61).

As immune sentinels, one of the primary roles of AMθ is to orchestrate immune responses by recruiting other immune cell types to the lung. In some models of acute lung injury(62, 63) (44)) including pneumonia induced by LPS or *P. aeruginosa pneumonia* infection, depletion of AMθ attenuates the recruitment of neutrophils to the lung indicating that AMθ can be a key source of neutrophil chemoattractants. Conversely, in other models, AMθ appear to play a greater role in the negative regulation of neutrophil migration in that the depletion of AMθ amplifies neutrophil recruitment (35, 42, 64-68). Neutrophils migrate in response to a number of chemoattractants(69) including CXCL2 (MIP-2 [mouse] / GROβ [human]) and CCL3 (MIP-1α), of which AMθ can be a major source(38, 70-72). Clodronate treatment resulted in a decrease in MIP-1α detected in BAL samples on day 10 following intramuscular ANDV challenge (**Fig. 5A**) and also resulted in a decrease in MIP-1α and MIP-2 on day 10 following intranasal challenge (**Fig.5B**). Surprisingly, the decrease in MIP-1α and MIP-2 in clodronate treated animals following intranasal challenge was accompanied by an increase in BAL neutrophils (**Fig. 5D**). Moreover, control encapsome treatment also resulted in decreases in MIP-1α and MIP-2 but recruitment of new AMθ rather than neutrophils. One possible explanation for this apparent paradox is that AMθ are an important source of MIP-1α and MIP-2 in the hamster but hamster neutrophils preferrentially respond to other chemokies, such as monocyte chemoattractant protein-1 (MCP-1) or KC, that may be more abundant in the absence of MIP-1α and MIP-2. Alternatively, MIP-1α and MIP-2 are preferentially secreted by cell types other than neutrophils in the hamster and the presence of AMθ suppresses neutrophil migration.

When alveolar macrophages are depleted, neutrophils freely migrate to the lung and act as a MIP-1α/MIP-2 "sponge" which soaks up free chemokine and reduces overall levels of bioavailable MIP-1α/MIP-2. A similar explanation could hold true for the decreased abundance of MIP-1α and MIP-2 following control encapsome treatment in which newly arrived AMθ act as the chemokine sponge. A closer analysis of the kinetics of MIP-1α and MIP-2 expression following alveolar macrophage depletion would be necessary to elucidate these possibilities. The expression of MIP-1α and MIP-2 on day 17 following intranasal ANDV challenge was similar across all treatment groups and substantially lower than that detected in ANDV alone hamsters on day 10. Whether this reflects decreased numbers of AMθ at day 17 versus day 10 or whether this is a natural attempt by the hamster to downregulate lung inflammation has yet to be determined. We believe this is first report of hamster-specific ELISA kits from a commercial vendor to be used with the Syrian hamster animal model. Given the brevity between the publishing of the Syrian hamster genome and the commercial availability of these ELISA kits , we can not discount the possibility that the cytokine expression patterns we see following clodrosome/encapsome treatments of ANDV-infected hamsters are related to the specifity of these kits. As such, while these measurements are reproducible, they should be interpreted within the context of the other parameters measured in these experiments (e.g. survival and AMθ numbers) until verified by other independent reports.

The potential role of VEGF in hantavirus disease pathogenesis has recently received a great deal of attention. In vitro, hantavirus infection sensitizes endothelial cells to VEGF rendering them hyperpermeable(73) in a process involving VE-cadherin(74, 75) and potentially β3 integrin(76). Similarly, increased levels of VEGF can be detected in pleural effluent from

patients with acute HPS(77) or in serum samples of acute HFRS patients(78). Alveolar macrophages are known to express VEGF during pulmonary infection and other forms of acute lung injury (79-84)suggesting that AMθ may respond similarly to hantavirus infection. Still, the fact that all hamsters infected with ANDV developed disease (**Fig. 2E and 3D**) suggested that AMθ do not significantly influence the expression of VEGF in hamsters. A significant increase in VEGF expression in the BAL of ANDV infected hamsters in late after infection (Day 17) was observed compared to normal hamsters but, as expected, the level or VEGF detected in the BAL of ANDV infected animals was nearly identical at later times after infection (Day 17) regardless of the presence or absence of AMθ (**Fig. 6**). However, contrary to our expectations, the depletion of AMθ resulted in a significant increase in the level of VEGF in the BAL of ANDV-infected hamsters at early times after intranasal challenge. Interestingly, when macrophages were depleted in animals prior to intranasal challenge, those animals developed disease faster than either untreated ANDV-infected animals or animals receiving control liposome treatments. This would seem to support the suggestion that VEGF contributes to hantavirus disease but it would argue that AMθ are not the sole source of VEGF. Pulmonary epithelial cells (85, 86) and neutrophils (87, 88) are other known sources of VEGF in the lung and could be contributing to the increased levels of VEGF seen in ANDV-infected hamsters. Epithelial cells are not the primary targets of hantaviruses and are thus unlikely to be expressing VEGF as a result of direct infection, but expression could be induced by inflammatory cytokines produced by other cells during infection or by hypoxia caused during HPS(89). Recently, a role for neutrophils in vascular leakage caused by HTNV infection of SCID mice has been suggested(90). Correspondingly, clodrosome treatment resulted in both a significant increase in BAL VEGF and

neutrophil numbers early after infection (Day10). Whether the depletion of neutrophils in hamsters alters hantavirus disease pathogenesis and the expression of VEGF in hamsters remains to be determined.

Small animal models are invaluable tools to study the pathogenesis of diseases caused by neglected infectious disease agents such as Andes virus. However, the utility of the hamster model, as well as the role of the immune response in hantavirus disease pathogenesis is contentious. Previously, we and others have demonstrated that the ablation of adaptive T and B cell responses to ANDV infection in hamsters does not alter the course of disease (91, 92). Here, using the Syrian hamster / Andes virus lethal disease model we demonstrate that another component of the immune system is not directly responsible for the HPS-like disease cause by ANDV in hamsters. The mechanism by which hantaviruses cause disease in humans and hamsters alike is not clear and many mechanisms of disease, both immune related and virus intrinsic, have been proposed. Making this more difficult is that aspects of the immune response to hantavirus infection are likely to be important for protection and viral clearance, even as they are viewed as contributing to disease. Still, it will be necessary to continue to evaluate other immune cell types, as we seek to understand their role in contributing to disease or protection following hantavirus infection.

ACKNOWLEDGMENTS

We thank Chris Mech for her excellent technical assistance in preparing and troubleshooting the hamster immunohistochemistry and pathology slides. We also thank Jimmy Fiallos for his excellent BSL-4 animal manipulation assistance.

This work was funded by the U.S. Army Medical Research and Material Command, Military Infectious Disease Research Program, Program Area T. Research reported in this publication was also supported by the National Institute of Allergy and Infectious Diseases of the National Institutes of Health under Award Number R01AI098933.

Opinions, interpretations, conclusions, and recommendations are those of the authors and not necessarily endorsed by the U.S. Army or the Department of Defense.

FIGURE LEGENDS

Figure 1. Identification and depletion of AMθ **in Syrian hamsters.** (**A**) AMθ from Syrian hamster BAL fluid were analyzed for the expression of the MARCO scavenger receptor by flow cytometry. Hamsters were treated intratracheally with Clodrosomes or control Encapsomes on days -3 and -1 prior to an 80 pfu ANDV i.m. challenge . 10 days post ANDV challenge, the ability of Encapasome or Clodrosome treatment to deplete AMθ was determined by analyzing the percent of $MARCO^{+}$ cells (**B**) or FSC^{hi}/SSC^{hi} cells (**C**) in hamster BAL samples. The percent of $MARCO^{+}$ cells or FSC^{hi}/SSC^{hi} cells was then quantified (**D**) (*, $P < 0.05$; ***, $P < 0.001$). (**E**) Staining of lungs of day 10 ANDV-infected hamsters with H&E (total magnification, ×400). 5 to 6 µm sections of one of the cranial lung lobes was stained with H&E to visually determine if the

number of alveolar macrophages is affected when treated with Clodrosomes, Encapsomes or when left untreated. Black arrows indicate alveolar macrophages.

Figure 2. Depletion of AMθ **does not prevent disease following intramuscular ANDV challenge.** Hamsters were treated intratracheally with Clodrosomes or control Encapsomes on days -3 and -1 or were left untreated. On day 0, all hamsters were challenged with 80 pfu ANDV by intramuscular infection. (**A**) 10 days post ANDV challenge, the number of AMθ was determined by flow cytometry by gating on FSC^{hi}/SSC^{hi} cells (as described in Fig. 1) in hamster BAL samples (**, $P < 0.01$; ****, $P < 0.0001$). (**B**) The depletion of AMθ did not prevent disease in hamsters. Lung tissue isolated from all hamsters 10 days post-challenge were evaluated for viral genome (**C**) by RT-PCR (not significant).

Figure 3. Depletion of AMθ **does not alter the localization of ANDV NP to CD31 positive endothelial cells.** 5 to 6 μm serial sections from one of the cranial lobes of Day 10 i.m. ANDV-infected hamsters treated with Clodrosomes (**A**), or Encapsomes (**B**), untreated ANDV-infected hamsters (**C**), or normal uninfected hamsters (**D**) were stained with antibodies specific for CD31 (DAB - brown) or ANDV NP (Alkaline phosphatase - red). ANDV NP staining colocalized to CD31 positive cells in adjacent serial sections. Normal hamster tissue remained negative for ANDV NP. No differences were seen in the pattern of CD31 and/or ANDV NP staining across treatment groups. (**E**) Alveolar macrophages from untreated ANDV-infected hamsters were evaluated for the presence of ANDV NP and CD31. All were found to be CD31 positive but no evidence of positive staining for ANDV NP was detected.

Figure 4. Depletion of alveolar macrophages does not prevent disease following intranasal ANDV challenge. Hamsters were treated intratracheally with Clodrosomes or control Encapsomes on days -3 and -1 or were left untreated. On day 0, all hamsters were challenged with 4000 pfu ANDV by intranasal infection. (**A**) 10 days and (**B**) 17 days post ANDV challenge, the number of AMθ was determined by flow cytometry by gating on FSC^{hi}/SSC^{hi} cells (as described in Fig. 1) in hamster BAL samples (**, $P < 0.01$; ***, $P < 0.001$; ns, not significant). (**C**) The number of AMθ on days 10 and 17 in untreated, ANDV-challenged hamsters was directly compared (**, $P < 0.01$). (**D**) The depletion of AMθ did not prevent disease in hamsters. All surviving animals seroconverted indicating that they had been exposed to virus (data not shown). Lung tissue isolated from all hamsters 10 and 17 post-challenge were evaluated for viral genome (E) by RT-PCR.

Figure 5. Depletion AMθ **alters TNFα expression but only early after intranasal ANDV challenge.** Hamsters were treated intratracheally with Clodrosomes or control Encapsomes on days -3 and -1 or were left untreated. On day 0, all hamsters were challenged with either 4000 pfu ANDV by intranasal infection or with 80 pfu ANDV by intramuscular infection. BAL samples were collected from all hamsters 10 and 17 days after intranasal challenge (**A**) or 10 days after intramuscular challenge (**B**) and TNFa expression was analyzed by ELISA. The depletion of AMθ resulted in increased TNFα levels 10 days after intranasal ANDV challenge (**A**) (**, $P < 0.01$) but did not affect TNFα levels 17 days after intranasal challenge or 10 days after intramuscular ANDV challenge (**B**). TNFα expression in BAL samples from untreated ANDV-challenged hamsters following either intranasal or intramuscular virus challenge were directly compared (**C**) (****, $P < 0.0001$).

Figure 6. Depletion of AMθ **alters neutrophil recruitment and neutrophil chemoattractant expression early after intranasal ANDV challenge.** BAL samples were collected from all hamsters 10 day s after intramuscular challenge (**A-C**) or 10 and 17 days after 4000 pfu intranasal ANDV challenge (**D-G**) and were analyzed for the presence of neutrophils by flow cytometry and MIP-1α and MIP-2 by ELISA. Both Clodrosome and Encapsome treatments resulted in a decrease in MIP-1α (**A**) but did not alter MIP-2 expression (**B**) or the number of neutrophils (**C**) compared to untreated hamsters after intramuscular challenge. Clodrosome and Encapsome treatments resulted in a decrease in both MIP-1α (**D**) and MIP-2 expression (**E**). Clodrosome treatment resulted in an increase in the number of neutrophils in hamster BAL fluid on day 10 (**F**) but not on day 17 (**G**) after intranasal challenge (*, $P < 0.05$; **, $P < 0.01$; ***, $P < 0.001$; ****, $P < 0.0001$; ns, not significant).

Figure 7. Depletion of AMθ **alters VEGF-A expression early after intranasal ANDV challenge.** BAL samples were collected from all hamsters 10 and 17 days after 4000 pfu intranasal ANDV challenge and were analyzed for the presence of VEGF-A by ELISA. Both Clodrosome and Encapsome treatments resulted in increased VEGF-A expression 10 days post ANDV challenge comparable to VEGF-A levels found in all hamsters 17 days post challenge (**, $P < 0.01$; ***, $P < 0.001$; ****, $P < 0.0001$; ns, not significant).

615 **References**

616

617 1. **Schmaljohn C, Hjelle B.** 1997. Hantaviruses: a global disease problem. Emerging infectious
618 diseases **3:**95-104.
619 2. **Peters CJ, Simpson GL, Levy H.** 1999. Spectrum of hantavirus infection: hemorrhagic fever with
620 renal syndrome and hantavirus pulmonary syndrome. Annual review of medicine **50:**531-545.
621 3. **Khan A, Khan AS.** 2003. Hantaviruses: a tale of two hemispheres. Panminerva medica **45:**43-51.
622 4. **Jonsson CB, Hooper J, Mertz G.** 2008. Treatment of hantavirus pulmonary syndrome. Antiviral
623 research **78:**162-169.
624 5. **Hooper JW, Ferro AM, Wahl-Jensen V.** 2008. Immune serum produced by DNA vaccination
625 protects hamsters against lethal respiratory challenge with Andes virus. Journal of virology
626 **82:**1332-1338.
627 6. **Hooper JW, Li D.** 2001. Vaccines against hantaviruses. Current topics in microbiology and
628 immunology **256:**171-191.
629 7. **Schmaljohn CSaJWH.** 2001. Bunyaviridae: The Viruses and Their Replication, p. 1581-1602,
630 Fields Virology, 4 ed. Lippincott, Williams, and Wilkins, Philadelphia, PA.
631 8. **Smith MR, Standiford TJ, Reddy RC.** 2007. PPARs in Alveolar Macrophage Biology. PPAR
632 research **2007:**23812.
633 9. **Kim HM, Lee YW, Lee KJ, Kim HS, Cho SW, van Rooijen N, Guan Y, Seo SH.** 2008. Alveolar
634 macrophages are indispensable for controlling influenza viruses in lungs of pigs. Journal of
635 virology **82:**4265-4274.
636 10. **Tumpey TM, Garcia-Sastre A, Taubenberger JK, Palese P, Swayne DE, Pantin-Jackwood MJ,**
637 **Schultz-Cherry S, Solorzano A, Van Rooijen N, Katz JM, Basler CF.** 2005. Pathogenicity of
638 influenza viruses with genes from the 1918 pandemic virus: functional roles of alveolar
639 macrophages and neutrophils in limiting virus replication and mortality in mice. Journal of
640 virology **79:**14933-14944.
641 11. **Farley KS, Wang L, Mehta S.** 2009. Septic pulmonary microvascular endothelial cell injury: role
642 of alveolar macrophage NADPH oxidase. American journal of physiology **296:**L480-488.
643 12. **Naidu BV, Woolley SM, Farivar AS, Thomas R, Fraga CH, Goss CH, Mulligan MS.** 2004. Early
644 tumor necrosis factor-alpha release from the pulmonary macrophage in lung ischemia-
645 reperfusion injury. The Journal of thoracic and cardiovascular surgery **127:**1502-1508.
646 13. **Sakamaki F, Ishizaka A, Urano T, Sayama K, Nakamura H, Terashima T, Waki Y, Soejima K,**
647 **Tasaka S, Sawafuji M, Kobayashi K, Yamaguchi K, Kanazawa M.** 2003. Attenuation by
648 intravenous 2-chloroadenosine of acute lung injury induced by live escherichia coli or latex
649 particles added to endotoxin in the neutropenic state. The Journal of laboratory and clinical
650 medicine **142:**128-135.
651 14. **Wallaert B, Bart F, Aerts C, Ouaissi A, Hatron PY, Tonnel AB, Voisin C.** 1988. Activated alveolar
652 macrophages in subclinical pulmonary inflammation in collagen vascular diseases. Thorax **43:**24-
653 30.
654 15. **Raychaudhuri SP, Nguyen CT, Raychaudhuri SK, Gershwin ME.** 2009. Incidence and nature of
655 infectious disease in patients treated with anti-TNF agents. Autoimmunity reviews.
656 16. **Beynon HL, Haskard DO, Davies KA, Haroutunian R, Walport MJ.** 1993. Combinations of low
657 concentrations of cytokines and acute agonists synergize in increasing the permeability of
658 endothelial monolayers. Clinical and experimental immunology **91:**314-319.

17. **Kerkar S, Williams M, Blocksom JM, Wilson RF, Tyburski JG, Steffes CP.** 2006. TNF-alpha and IL-1beta increase pericyte/endothelial cell co-culture permeability. J Surg Res **132:**40-45.
18. **Kotowicz K, Callard RE, Klein NJ, Jacobs MG.** 2004. Interleukin-4 increases the permeability of human endothelial cells in culture. Clin Exp Allergy **34:**445-449.
19. **Maruo N, Morita I, Shirao M, Murota S.** 1992. IL-6 increases endothelial permeability in vitro. Endocrinology **131:**710-714.
20. **Nooteboom A, Bleichrodt RP, Hendriks T.** 2006. Modulation of endothelial monolayer permeability induced by plasma obtained from lipopolysaccharide-stimulated whole blood. Clinical and experimental immunology **144:**362-369.
21. **Mori M, Rothman AL, Kurane I, Montoya JM, Nolte KB, Norman JE, Waite DC, Koster FT, Ennis FA.** 1999. High levels of cytokine-producing cells in the lung tissues of patients with fatal hantavirus pulmonary syndrome. The Journal of infectious diseases **179:**295-302.
22. **Linderholm M, Ahlm C, Settergren B, Waage A, Tarnvik A.** 1996. Elevated plasma levels of tumor necrosis factor (TNF)-alpha, soluble TNF receptors, interleukin (IL)-6, and IL-10 in patients with hemorrhagic fever with renal syndrome. The Journal of infectious diseases **173:**38-43.
23. **Li W, Klein SL.** 2012. Seoul virus-infected rat lung endothelial cells and alveolar macrophages differ in their ability to support virus replication and induce regulatory T cell phenotypes. Journal of virology **86:**11845-11855.
24. **Khaiboullina SF, Netski DM, Krumpe P, St Jeor SC.** 2000. Effects of tumor necrosis factor alpha on sin nombre virus infection in vitro. Journal of virology **74:**11966-11971.
25. **Zaki SR, Greer PW, Coffield LM, Goldsmith CS, Nolte KB, Foucar K, Feddersen RM, Zumwalt RE, Miller GL, Khan AS, et al.** 1995. Hantavirus pulmonary syndrome. Pathogenesis of an emerging infectious disease. The American journal of pathology **146:**552-579.
26. **Gizzi M, Delaere B, Weynand B, Clement J, Maes P, Vergote V, Laenen L, Hjelle B, Verroken A, Dive A, Michaux I, Evrard P, Creytens D, Bulpa P.** 2013. Another case of "European hantavirus pulmonary syndrome" with severe lung, prior to kidney, involvement, and diagnosed by viral inclusions in lung macrophages. European journal of clinical microbiology & infectious diseases : official publication of the European Society of Clinical Microbiology **32:**1341-1345.
27. **Hooper JW, Larsen T, Custer DM, Schmaljohn CS.** 2001. A lethal disease model for hantavirus pulmonary syndrome. Virology **289:**6-14.
28. **Padula PJ, Colavecchia SB, Martinez VP, Gonzalez Della Valle MO, Edelstein A, Miguel SD, Russi J, Riquelme JM, Colucci N, Almiron M, Rabinovich RD.** 2000. Genetic diversity, distribution, and serological features of hantavirus infection in five countries in South America. Journal of clinical microbiology **38:**3029-3035.
29. **Palecanda A, Paulauskis J, Al-Mutairi E, Imrich A, Qin G, Suzuki H, Kodama T, Tryggvason K, Koziel H, Kobzik L.** 1999. Role of the scavenger receptor MARCO in alveolar macrophage binding of unopsonized environmental particles. The Journal of experimental medicine **189:**1497-1506.
30. **Wahl-Jensen V, Chapman J, Asher L, Fisher R, Zimmerman M, Larsen T, Hooper JW.** 2007. Temporal analysis of Andes virus and Sin Nombre virus infections of Syrian hamsters. Journal of virology **81:**7449-7462.
31. **Nemmar A, Nemery B, Hoet PH, Van Rooijen N, Hoylaerts MF.** 2005. Silica particles enhance peripheral thrombosis: key role of lung macrophage-neutrophil cross-talk. American journal of respiratory and critical care medicine **171:**872-879.
32. **Ochs M, Nyengaard JR, Jung A, Knudsen L, Voigt M, Wahlers T, Richter J, Gundersen HJ.** 2004. The number of alveoli in the human lung. American journal of respiratory and critical care medicine **169:**120-124.
33. **Pollmacher J, Figge MT.** 2014. Agent-based model of human alveoli predicts chemotactic signaling by epithelial cells during early Aspergillus fumigatus infection. PloS one **9:**e111630.

34. **Holt PG, Strickland DH, Wikstrom ME, Jahnsen FL.** 2008. Regulation of immunological homeostasis in the respiratory tract. Nature reviews. Immunology **8:**142-152.
35. **Rivera R, Hutchens M, Luker KE, Sonstein J, Curtis JL, Luker GD.** 2007. Murine alveolar macrophages limit replication of vaccinia virus. Virology **363:**48-58.
36. **Benoit A, Huang Y, Proctor J, Rowden G, Anderson R.** 2006. Effects of alveolar macrophage depletion on liposomal vaccine protection against respiratory syncytial virus (RSV). Clinical and experimental immunology **145:**147-154.
37. **Reed JL, Brewah YA, Delaney T, Welliver T, Burwell T, Benjamin E, Kuta E, Kozhich A, McKinney L, Suzich J, Kiener PA, Avendano L, Velozo L, Humbles A, Welliver RC, Sr., Coyle AJ.** 2008. Macrophage impairment underlies airway occlusion in primary respiratory syncytial virus bronchiolitis. The Journal of infectious diseases **198:**1783-1793.
38. **Pribul PK, Harker J, Wang B, Wang H, Tregoning JS, Schwarze J, Openshaw PJ.** 2008. Alveolar macrophages are a major determinant of early responses to viral lung infection but do not influence subsequent disease development. Journal of virology **82:**4441-4448.
39. **Murphy EA, Davis JM, McClellan JL, Carmichael MD, Rooijen NV, Gangemi JD.** 2011. Susceptibility to infection and inflammatory response following influenza virus (H1N1, A/PR/8/34) challenge: role of macrophages. J Interferon Cytokine Res **31:**501-508.
40. **Schneider C, Nobs SP, Heer AK, Kurrer M, Klinke G, van Rooijen N, Vogel J, Kopf M.** 2014. Alveolar macrophages are essential for protection from respiratory failure and associated morbidity following influenza virus infection. PLoS pathogens **10:**e1004053.
41. **Kolli D, Gupta MR, Sbrana E, Velayutham TS, Chao H, Casola A, Garofalo RP.** 2014. Alveolar macrophages contribute to the pathogenesis of human metapneumovirus infection while protecting against respiratory syncytial virus infection. American journal of respiratory cell and molecular biology **51:**502-515.
42. **Kooguchi K, Hashimoto S, Kobayashi A, Kitamura Y, Kudoh I, Wiener-Kronish J, Sawa T.** 1998. Role of alveolar macrophages in initiation and regulation of inflammation in Pseudomonas aeruginosa pneumonia. Infection and immunity **66:**3164-3169.
43. **Duan M, Li WC, Vlahos R, Maxwell MJ, Anderson GP, Hibbs ML.** 2012. Distinct macrophage subpopulations characterize acute infection and chronic inflammatory lung disease. J Immunol **189:**946-955.
44. **Naidu BV, Krishnadasan B, Farivar AS, Woolley SM, Thomas R, Van Rooijen N, Verrier ED, Mulligan MS.** 2003. Early activation of the alveolar macrophage is critical to the development of lung ischemia-reperfusion injury. The Journal of thoracic and cardiovascular surgery **126:**200-207.
45. **Ferreira CS, Frenzke M, Leonard VH, Welstead GG, Richardson CD, Cattaneo R.** 2010. Measles virus infection of alveolar macrophages and dendritic cells precedes spread to lymphatic organs in transgenic mice expressing human signaling lymphocytic activation molecule (SLAM, CD150). Journal of virology **84:**3033-3042.
46. **Copenhaver AM, Casson CN, Nguyen HT, Fung TC, Duda MM, Roy CR, Shin S.** 2014. Alveolar macrophages and neutrophils are the primary reservoirs for Legionella pneumophila and mediate cytosolic surveillance of type IV secretion. Infection and immunity **82:**4325-4336.
47. **Hartwig SM, Holman KM, Varga SM.** 2014. Depletion of alveolar macrophages ameliorates virus-induced disease following a pulmonary coronavirus infection. PloS one **9:**e90720.
48. **Raftery MJ, Lalwani P, Krautkrmer E, Peters T, Scharffetter-Kochanek K, Kruger R, Hofmann J, Seeger K, Kruger DH, Schonrich G.** 2014. beta2 integrin mediates hantavirus-induced release of neutrophil extracellular traps. The Journal of experimental medicine **211:**1485-1497.

49. **Hodge S, Hodge G, Ahern J, Jersmann H, Holmes M, Reynolds PN.** 2007. Smoking alters alveolar macrophage recognition and phagocytic ability: implications in chronic obstructive pulmonary disease. American journal of respiratory cell and molecular biology **37:**748-755.
50. **Gil M, McCormack FX, Levine AM.** 2009. Surfactant protein A modulates cell surface expression of CR3 on alveolar macrophages and enhances CR3-mediated phagocytosis. The Journal of biological chemistry **284:**7495-7504.
51. **Simmons G, Reeves JD, Grogan CC, Vandenberghe LH, Baribaud F, Whitbeck JC, Burke E, Buchmeier MJ, Soilleux EJ, Riley JL, Doms RW, Bates P, Pohlmann S.** 2003. DC-SIGN and DC-SIGNR bind ebola glycoproteins and enhance infection of macrophages and endothelial cells. Virology **305:**115-123.
52. **Gibb TR, Norwood DA, Jr., Woollen N, Henchal EA.** 2002. Viral replication and host gene expression in alveolar macrophages infected with Ebola virus (Zaire strain). Clinical and diagnostic laboratory immunology **9:**19-27.
53. **Barreto DF, Takiya CM, Schatzmayr HG, Nogueira RM, Farias-Filho Jda C, Barth OM.** 2007. Histopathological and ultrastructural aspects of mice lungs experimentally infected with dengue virus serotype 2. Memorias do Instituto Oswaldo Cruz **102:**175-182.
54. **Povoa TF, Alves AM, Oliveira CA, Nuovo GJ, Chagas VL, Paes MV.** 2014. The pathology of severe dengue in multiple organs of human fatal cases: histopathology, ultrastructure and virus replication. PloS one **9:**e83386.
55. **Hussell T, Bell TJ.** 2014. Alveolar macrophages: plasticity in a tissue-specific context. Nature reviews. Immunology **14:**81-93.
56. **Thepen T, Van Rooijen N, Kraal G.** 1989. Alveolar macrophage elimination in vivo is associated with an increase in pulmonary immune response in mice. The Journal of experimental medicine **170:**499-509.
57. **Strickland DH, Thepen T, Kees UR, Kraal G, Holt PG.** 1993. Regulation of T-cell function in lung tissue by pulmonary alveolar macrophages. Immunology **80:**266-272.
58. **Holt PG, Oliver J, Bilyk N, McMenamin C, McMenamin PG, Kraal G, Thepen T.** 1993. Downregulation of the antigen presenting cell function(s) of pulmonary dendritic cells in vivo by resident alveolar macrophages. The Journal of experimental medicine **177:**397-407.
59. **Gwinn MR, Vallyathan V.** 2006. Respiratory burst: role in signal transduction in alveolar macrophages. Journal of toxicology and environmental health. Part B, Critical reviews **9:**27-39.
60. **Underhill DM, Ozinsky A.** 2002. Phagocytosis of microbes: complexity in action. Annual review of immunology **20:**825-852.
61. **Bilyk N, Holt PG.** 1995. Cytokine modulation of the immunosuppressive phenotype of pulmonary alveolar macrophage populations. Immunology **86:**231-237.
62. **Maus UA, Koay MA, Delbeck T, Mack M, Ermert M, Ermert L, Blackwell TS, Christman JW, Schlondorff D, Seeger W, Lohmeyer J.** 2002. Role of resident alveolar macrophages in leukocyte traffic into the alveolar air space of intact mice. American journal of physiology **282:**L1245-1252.
63. **Cohen TS, Prince AS.** 2013. Activation of inflammasome signaling mediates pathology of acute P. aeruginosa pneumonia. The Journal of clinical investigation **123:**1630-1637.
64. **Broug-Holub E, Toews GB, van Iwaarden JF, Strieter RM, Kunkel SL, Paine R, 3rd, Standiford TJ.** 1997. Alveolar macrophages are required for protective pulmonary defenses in murine Klebsiella pneumonia: elimination of alveolar macrophages increases neutrophil recruitment but decreases bacterial clearance and survival. Infection and immunity **65:**1139-1146.
65. **Cheung DO, Halsey K, Speert DP.** 2000. Role of pulmonary alveolar macrophages in defense of the lung against Pseudomonas aeruginosa. Infection and immunity **68:**4585-4592.

66. **Machado-Aranda D, M VS, Yu B, Dolgachev V, Hemmila MR, Raghavendran K.** 2014. Alveolar macrophage depletion increases the severity of acute inflammation following nonlethal unilateral lung contusion in mice. The journal of trauma and acute care surgery **76:**982-990.
67. **Nakamura T, Abu-Dahab R, Menger MD, Schafer U, Vollmar B, Wada H, Lehr CM, Schafers HJ.** 2005. Depletion of alveolar macrophages by clodronate-liposomes aggravates ischemia-reperfusion injury of the lung. The Journal of heart and lung transplantation : the official publication of the International Society for Heart Transplantation **24:**38-45.
68. **Elder A, Johnston C, Gelein R, Finkelstein J, Wang Z, Notter R, Oberdorster G.** 2005. Lung inflammation induced by endotoxin is enhanced in rats depleted of alveolar macrophages with aerosolized clodronate. Experimental lung research **31:**527-546.
69. **Sadik CD, Kim ND, Luster AD.** 2011. Neutrophils cascading their way to inflammation. Trends Immunol **32:**452-460.
70. **Hashimoto S, Pittet JF, Hong K, Folkesson H, Bagby G, Kobzik L, Frevert C, Watanabe K, Tsurufuji S, Wiener-Kronish J.** 1996. Depletion of alveolar macrophages decreases neutrophil chemotaxis to Pseudomonas airspace infections. The American journal of physiology **270:**L819-828.
71. **Fujimoto J, Wiener-Kronish JP, Hashimoto S, Sawa T.** 2002. Effects of Cl2MDP-encapsulating liposomes in a murine model of Pseudomonas aeruginosa-induced sepsis. Journal of liposome research **12:**239-257.
72. **Zhao M, Fernandez LG, Doctor A, Sharma AK, Zarbock A, Tribble CG, Kron IL, Laubach VE.** 2006. Alveolar macrophage activation is a key initiation signal for acute lung ischemia-reperfusion injury. American journal of physiology **291:**L1018-1026.
73. **Gavrilovskaya IN, Gorbunova EE, Mackow NA, Mackow ER.** 2008. Hantaviruses direct endothelial cell permeability by sensitizing cells to the vascular permeability factor VEGF, while angiopoietin 1 and sphingosine 1-phosphate inhibit hantavirus-directed permeability. Journal of virology **82:**5797-5806.
74. **Gorbunova E, Gavrilovskaya IN, Mackow ER.** Pathogenic hantaviruses Andes virus and Hantaan virus induce adherens junction disassembly by directing vascular endothelial cadherin internalization in human endothelial cells. Journal of virology **84:**7405-7411.
75. **Shrivastava-Ranjan P, Rollin PE, Spiropoulou CF.** 2010. Andes virus disrupts the endothelial cell barrier by induction of vascular endothelial growth factor and downregulation of VE-cadherin. Journal of virology **84:**11227-11234.
76. **Wang W, Zhang Y, Li Y, Pan L, Bai L, Zhuang Y, Huang CX, Wang JP, Yu HT, Wei X, Jiang W, Nan YY, Yang DQ, Su WJ, Wang PZ, Bai XF.** 2012. Dysregulation of the beta3 integrin-VEGFR2 complex in Hantaan virus-directed hyperpermeability upon treatment with VEGF. Archives of virology **157:**1051-1061.
77. **Gavrilovskaya I, Gorbunova E, Koster F, Mackow E.** Elevated VEGF Levels in Pulmonary Edema Fluid and PBMCs from Patients with Acute Hantavirus Pulmonary Syndrome. Adv Virol **2012:**674360.
78. **Li Y, Wang W, Wang JP, Pan L, Zhang Y, Yu HT, Jiang W, Wang PZ, Bai XF.** 2012. Elevated vascular endothelial growth factor levels induce hyperpermeability of endothelial cells in hantavirus infection. The Journal of international medical research **40:**1812-1821.
79. **Medford AR, Douglas SK, Godinho SI, Uppington KM, Armstrong L, Gillespie KM, van Zyl B, Tetley TD, Ibrahim NB, Millar AB.** 2009. Vascular Endothelial Growth Factor (VEGF) isoform expression and activity in human and murine lung injury. Respiratory research **10:**27.
80. **Maretta M, Toth S, Jonecova Z, Kruzliak P, Kubatka P, Pingorova S, Vesela J.** 2014. Immunohistochemical expression of MPO, CD163 and VEGF in inflammatory cells in acute

respiratory distress syndrome: a case report. International journal of clinical and experimental pathology **7:**4539-4544.

81. **Song C, Ma H, Yao C, Tao X, Gan H.** 2012. Alveolar macrophage-derived vascular endothelial growth factor contributes to allergic airway inflammation in a mouse asthma model. Scandinavian journal of immunology **75:**599-605.
82. **Nishigaki Y, Fujiuchi S, Fujita Y, Yamazaki Y, Sato M, Yamamoto Y, Takeda A, Fujikane T, Shimizu T, Kikuchi K.** 2006. Increased serum level of vascular endothelial growth factor in Mycobacterium avium complex infection. Respirology **11:**407-413.
83. **Shariati F, Perez-Arellano JL, Lopez-Aban J, El Behairy AM, Muro A.** 2010. Role of angiogenic factors in acute experimental Strongyloides venezuelensis infection. Parasite immunology **32:**430-439.
84. **Shariati F, Perez-Arellano JL, Carranza C, Lopez-Aban J, Vicente B, Arefi M, Muro A.** 2011. Evaluation of the role of angiogenic factors in the pathogenesis of schistosomiasis. Experimental parasitology **128:**44-49.
85. **Koyama S, Sato E, Nomura H, Kubo K, Miura M, Yamashita T, Nagai S, Izumi T.** 1999. The potential of various lipopolysaccharides to release monocyte chemotactic activity from lung epithelial cells and fibroblasts. Eur Respir J **14:**545-552.
86. **Koyama S, Sato E, Tsukadaira A, Haniuda M, Numanami H, Kurai M, Nagai S, Izumi T.** 2002. Vascular endothelial growth factor mRNA and protein expression in airway epithelial cell lines in vitro. Eur Respir J **20:**1449-1456.
87. **Tan KW, Chong SZ, Wong FH, Evrard M, Tan SM, Keeble J, Kemeny DM, Ng LG, Abastado JP, Angeli V.** 2013. Neutrophils contribute to inflammatory lymphangiogenesis by increasing VEGF-A bioavailability and secreting VEGF-D. Blood **122:**3666-3677.
88. **Taichman NS, Young S, Cruchley AT, Taylor P, Paleolog E.** 1997. Human neutrophils secrete vascular endothelial growth factor. Journal of leukocyte biology **62:**397-400.
89. **Pham I, Uchida T, Planes C, Ware LB, Kaner R, Matthay MA, Clerici C.** 2002. Hypoxia upregulates VEGF expression in alveolar epithelial cells in vitro and in vivo. American journal of physiology **283:**L1133-1142.
90. **Koma T, Yoshimatsu K, Nagata N, Sato Y, Shimizu K, Yasuda SP, Amada T, Nishio S, Hasegawa H, Arikawa J.** 2014. Neutrophil depletion suppresses pulmonary vascular hyperpermeability and occurrence of pulmonary edema caused by hantavirus infection in C.B-17 SCID mice. Journal of virology **88:**7178-7188.
91. **Hammerbeck CD, Hooper JW.** 2011. T cells are not required for pathogenesis in the Syrian hamster model of hantavirus pulmonary syndrome. Journal of virology **85:**9929-9944.
92. **Prescott J, Safronetz D, Haddock E, Robertson S, Scott D, Feldmann H.** 2013. The adaptive immune response does not influence hantavirus disease or persistence in the Syrian hamster. Immunology **140:**168-178.

Figure 1.

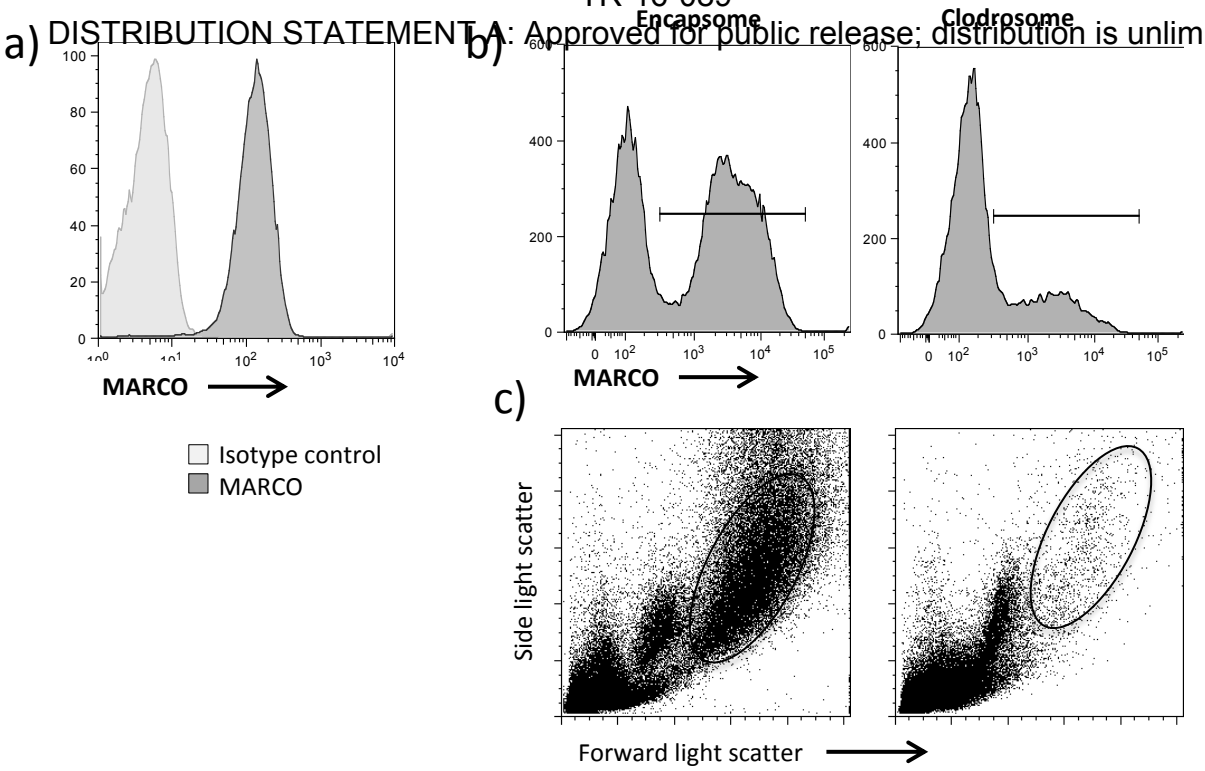

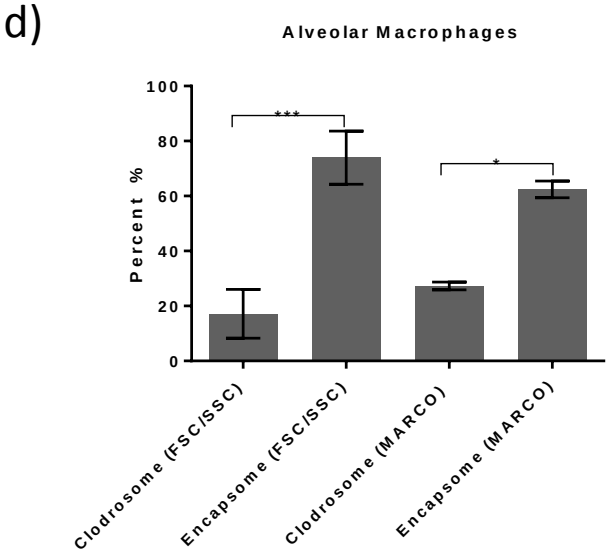

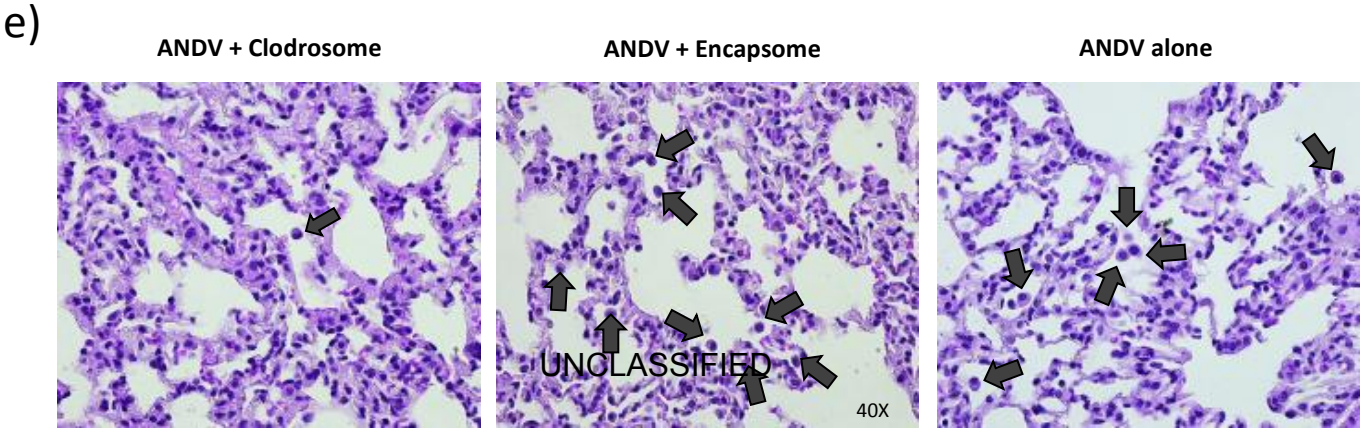

a)

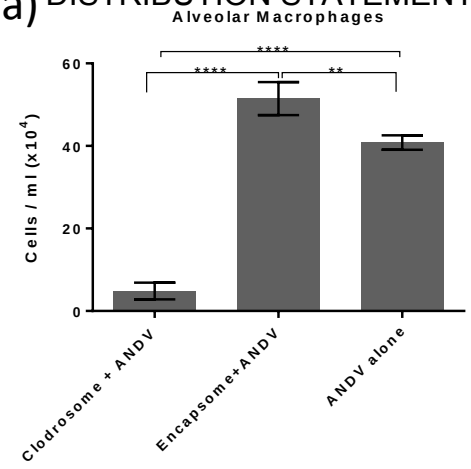
Alveolar Macrophages
Cells / ml (x10^4)
60
40
20
0
****
****
**
Clodrosome + ANDV
Encapsome+ANDV
ANDV alone

b)

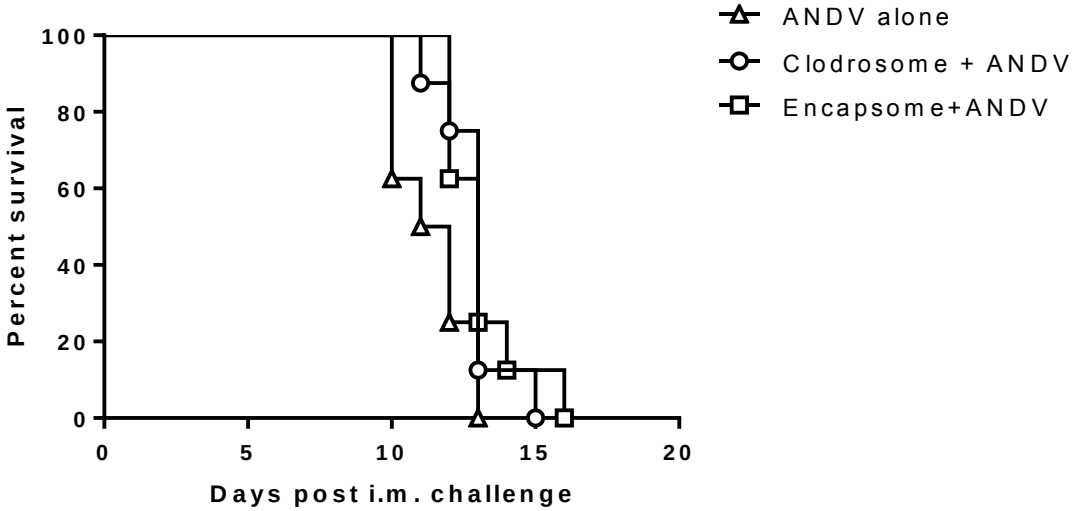
Percent survival
100
80
60
40
20
0
0
5
10
15
20
Days post i.m. challenge
ANDV alone
Clodrosome + ANDV
Encapsome+ANDV

c)

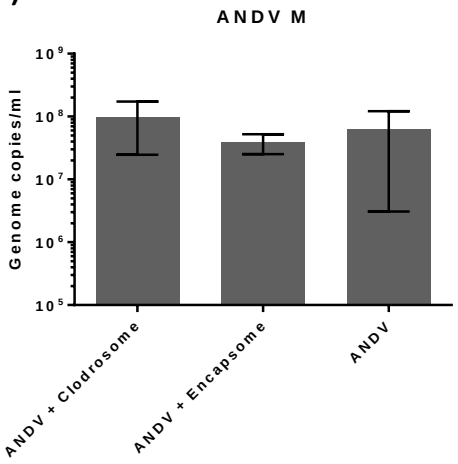
ANDV M
Genome copies/ml
10^9
10^8
10^7
10^6
10^5
ANDV + Clodrosome
ANDV + Encapsome
ANDV

Figure 3.

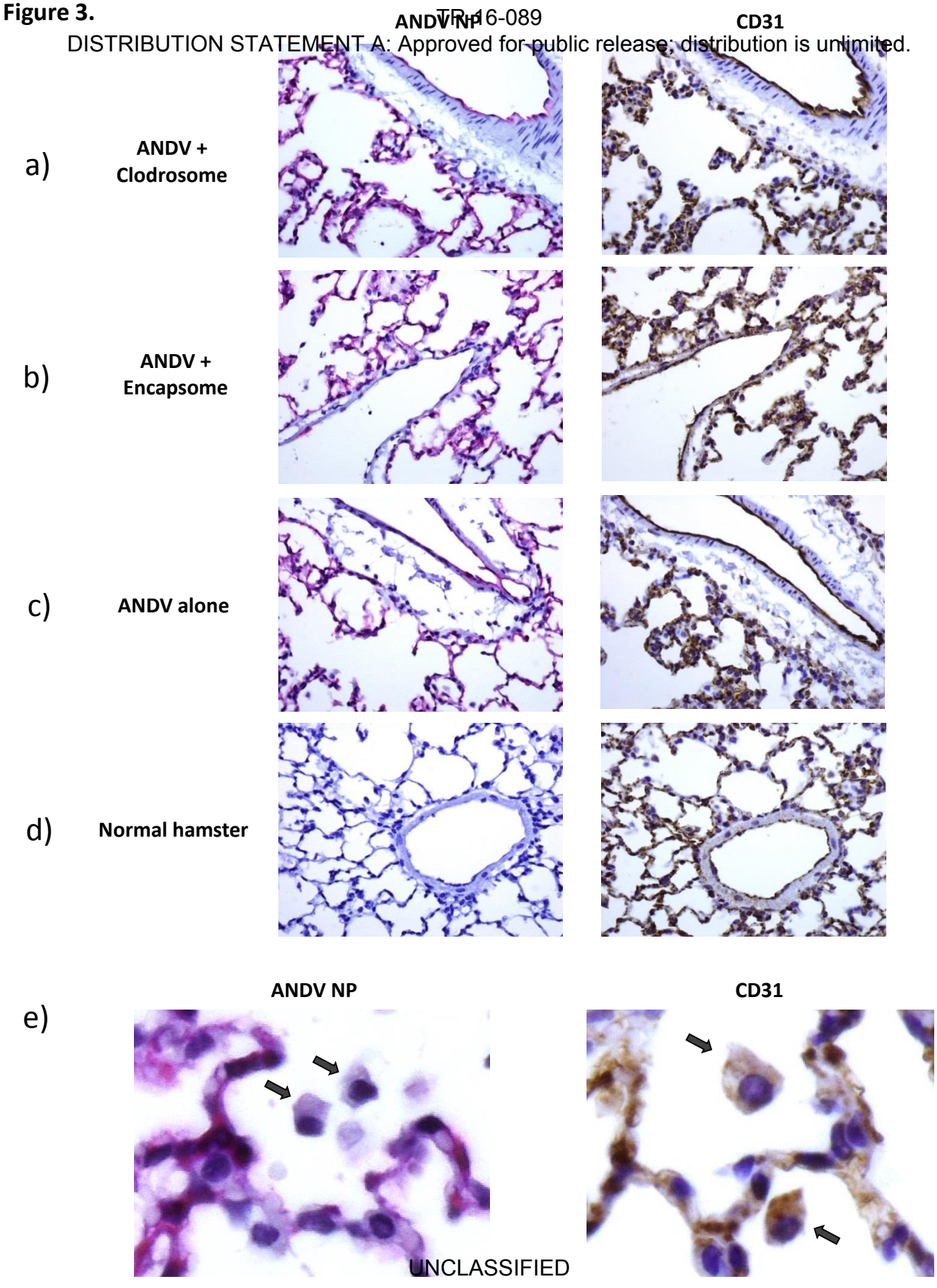

Figure 4.

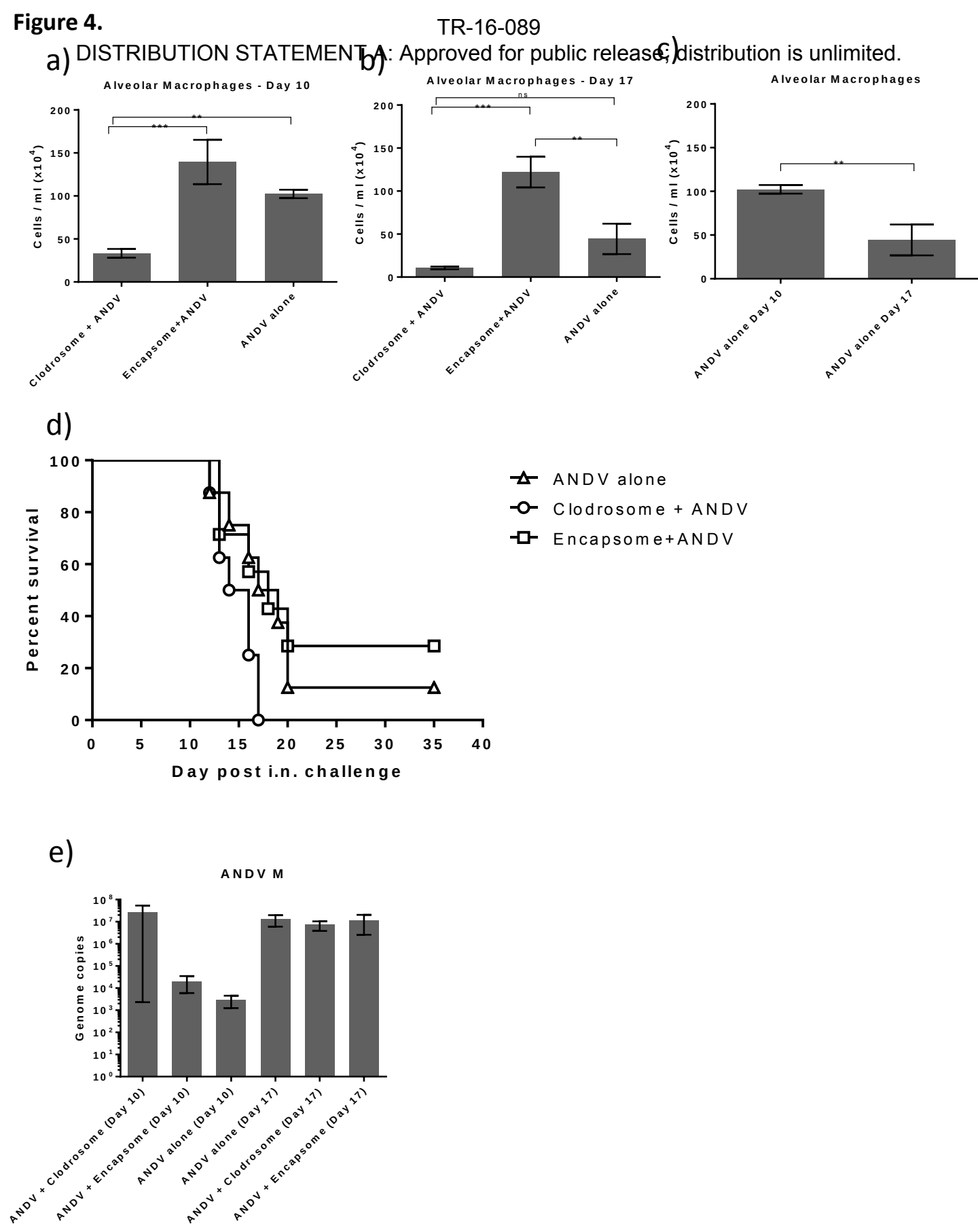

Figure 5.

a)

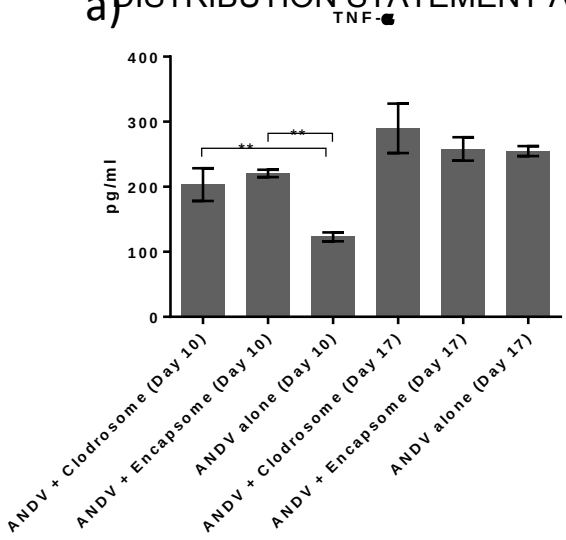

b)

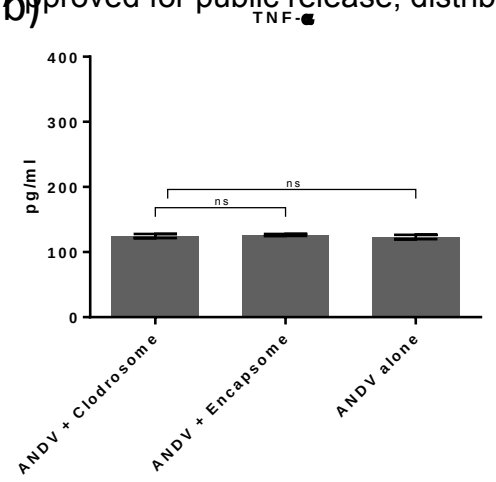

c)

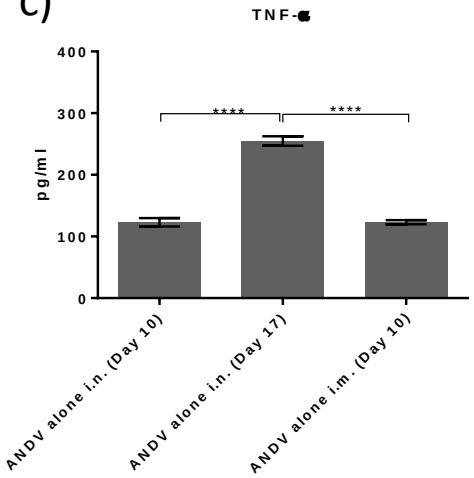

a)

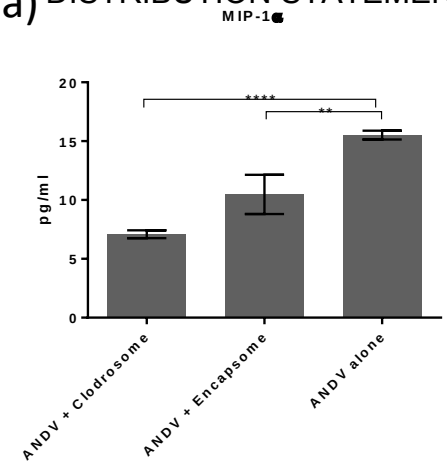
MIP-1α
pg/ml
ANDV + Clodrosome
ANDV + Encapsome
ANDV alone

b)

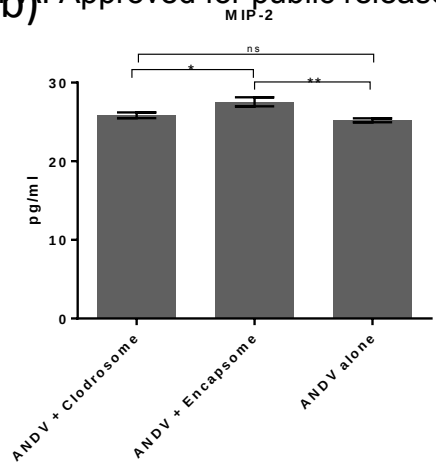
MIP-2
pg/ml
ns
ANDV + Clodrosome
ANDV + Encapsome
ANDV alone

c)

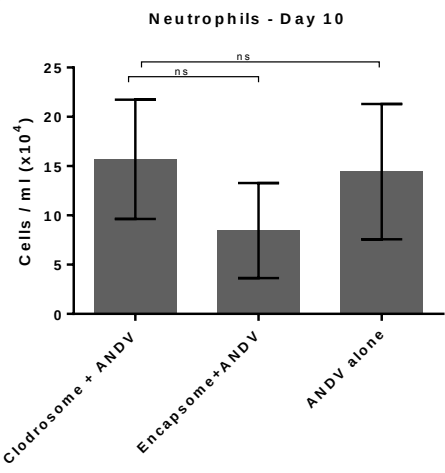
Neutrophils - Day 10
Cells / ml (x10^4)
ns
Clodrosome + ANDV
Encapsome+ANDV
ANDV alone

d)

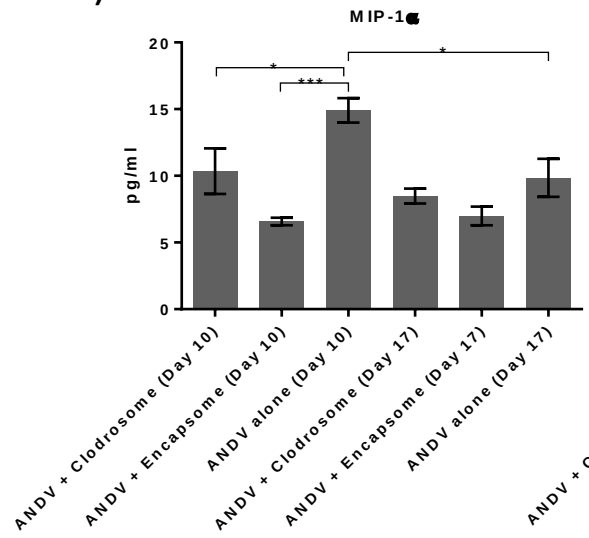
MIP-1α
pg/ml
ANDV + Clodrosome (Day 10)
ANDV + Encapsome (Day 10)
ANDV alone (Day 10)
ANDV + Clodrosome (Day 17)
ANDV + Encapsome (Day 17)
ANDV alone (Day 17)

e)

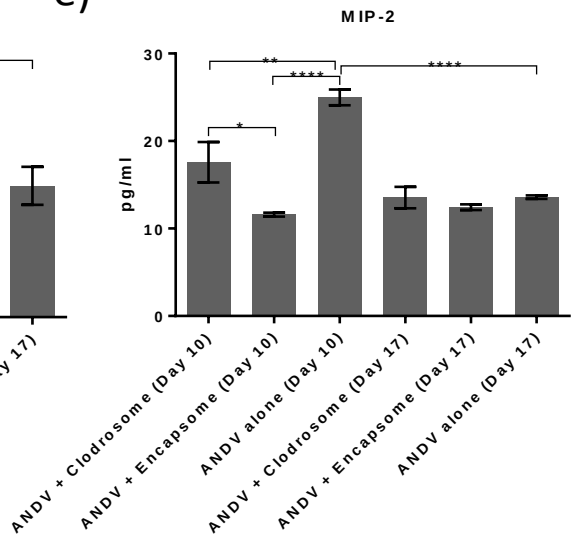
MIP-2
pg/ml
ANDV + Clodrosome (Day 10)
ANDV + Encapsome (Day 10)
ANDV alone (Day 10)
ANDV + Clodrosome (Day 17)
ANDV + Encapsome (Day 17)
ANDV alone (Day 17)

f)

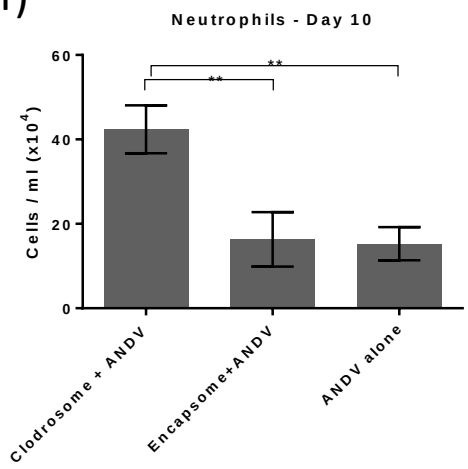
Neutrophils - Day 10
Cells / ml (x10^4)
Clodrosome + ANDV
Encapsome+ANDV
ANDV alone

g)

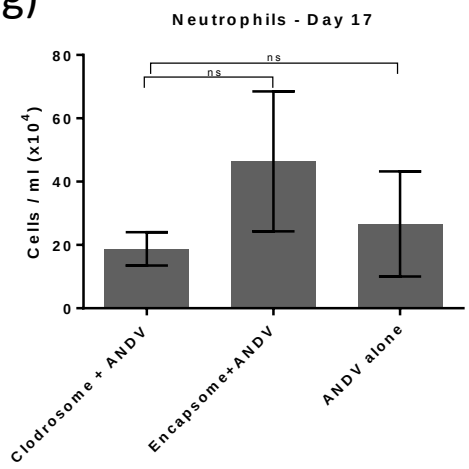
Neutrophils - Day 17
Cells / ml (x10^4)
ns
Clodrosome + ANDV
Encapsome+ANDV
ANDV alone

Figure 7.

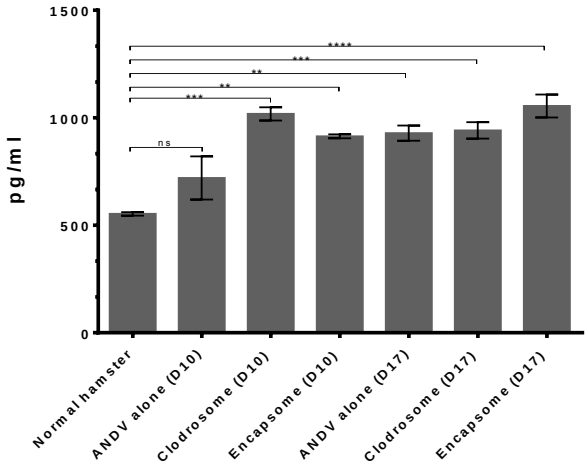
1500
1000
500
0
pg/ml
****
***
**
**
***
n.s
Normal hamster
ANDV alone (D10)
Clodrosome (D10)
Encapsome (D10)
ANDV alone (D17)
Clodrosome (D17)
Encapsome (D17)